

# Collective Pitch Control with Active Tower Damping of a Wind Turbine by Using a Nonlinear PID Approach

Adrian Gambier\* and Yul Yunazwin Nazaruddin<sup>+</sup>

\**Fraunhofer IWES, Fraunhofer Institute for Wind Energy Systems, 27572 Bremerhaven, Germany*  
(Tel: +49 471 14290-375; e-mail: [adrian.gambier@iwes.fraunhofer.de](mailto:adrian.gambier@iwes.fraunhofer.de))

<sup>+</sup>*Control Research Group, Institut Teknologi Bandung, Bandung 40132, Indonesia*  
(Tel: +62-22-2512971, e-mail: [yul@tf.itb.ac.id](mailto:yul@tf.itb.ac.id))

**Abstract:** The present work describes the results obtained from a nonlinear PID control (NPID) approach for the pitch control with top tower active damping of a large wind turbine. The control algorithm is implemented by using a well-known approach based on hyperbolic secant functions. A nonlinear PID controller and a nonlinear P controller are used for the collective pitch control and the active tower damping, respectively. As simulation platform, the 5-MW reference turbine developed by NREL and the software FAST are used. Results show that the NPID approach can provide significant improvements in the control performance in comparison to the classic control approach, in particular when the wind speed goes far from its rated value.

**Keywords:** Wind turbine control, pitch control, nonlinear PID

## 1. INTRODUCTION

The standard control strategy for wind turbines in Region III (i.e. wind speed overrated) consists in maintaining the rotor speed constant by pitching simultaneously all blades the same pitch angle, i.e. by doing collective pitch control (CPC, see e.g. (Burton, et al., 2011)). In (Bossanyi, 2000), it is proposed to modify the blade pitch angle provided by the collective pitch controller by using the feedback of the fore-aft tower oscillation speed, which is obtained by integrating the measured tower acceleration. This procedure actively damps tower oscillations. This approach has also been explored in (Leithead & Domínguez, 2004) (Bossanyi, 2003), (Wright & Fingersh, 2008), (Murtagh, et al., 2008) and (Gambier, 2017). The pitch adjustment to damp actively the tower fore-aft motion can be seen as an additional proportional (P) controller that detunes lightly the CPC.

On the other hand, the control technology of wind turbines has been dominated by the implementation of PI/PID algorithms (Proportional, Integral, and Derivative). However, with the advent of large sized wind turbines, which are characterized by flexible structures, nonlinearities in the pitch actuators as well as in the aerodynamics, and many operation points, which are depending on a stochastic variable, i.e. the wind speed, the standard control approaches become progressively insufficient for maintaining an acceptable degree of control performance.

An alternative is to implement a PID control system with nonlinear adjusting of the controller parameters (see e.g. (Shahruz & Schwartz, 1993) and (Xu, et al., 1995)). This approach, which usually is called NPID (Nonlinear PID), has successfully been used in Robotic but it is still not applied for the control of wind turbines. Hence, the present work reports the results of a NPID approach to the pitch control system of a multi-megawatt wind turbine, which consists of a collective pitch control and the active tower damping control.

The paper is organized as follows: In Section 2, the NPID is introduced following (Isayed & Hawwa, 2007). In Section 3, the

control problem of the wind turbine in case of overrated wind speed is presented. The implementation of the control approach for the wind turbine is the subject of Section 4. Section 5 is dedicated to present the simulation experiments and to analyse the results. Finally, the conclusion are drawn in Section 6.

## 2. NONLINEAR PID CONTROL

The nonlinear PID (NPID) controller is a PID controller, where the constant parameters are pre-multiplied by nonlinear functions. This concept is introduced in the following.

### 2.1 Standard PID Controller

The standard PID controller is well known and there is copious literature about it (see e.g. (Åström & Hagglund, 2005)). It is included here for the sake of completeness and as a support for the introduction of the NPID. The can be found including reference weighting, filtering of the derivative and anti-windup as

$$U(s) = K_p [bR(s) - Y(s)] + \frac{1}{s} [K_i E(s) + (1/T_d) [U(s)] - \bar{U}(s)] - \frac{K_d s}{1 + T_1 s} Y(s), \quad (1)$$

where  $K_p$ ,  $K_i$ , and  $K_d$  are the proportional, integral, and derivative gains, respectively.  $b$  is a weighting factor between 0 and 1 for the reference signals  $R$  and the derivative part includes a first order filter, whose time constant is  $T_1$ . In addition, the integrative part includes an anti-windup mechanism with the tracking-time constant  $T_a$ .

### 2.2 Simple Nonlinear PID

The most simple approach for a nonlinear PID controller consists of a nonlinear function  $f(e)$  of the error in cascade with a linear fixed-gain PID controller (e.g. (Seraji, 1998) and (Su, et al., 2005)). The nonlinear function is then bounded in the region  $0 \leq f(e) \leq f_{\max}$ . There are several possible functions to be used here. The most common are smooth sigmoidal functions, hyperbolic functions and bounded piecewise-linear functions (Seraji, 1998). The nonlinear function is usually described as

$$f(e) = K_0 + K_1 [g(e) - 1], \quad (2)$$

where  $1 \leq g(e) \leq 2$  such that  $f_{\max} = K_0 + K_1$  when  $g(e) = 2$  and  $f_{\min} = K_0$  when  $g(e) = 1$ . The value  $g(e) = 1$  should be obtained for  $e = 0$  whereas the value  $g(e) = 2$  for  $e = \pm\infty$ . Hence,  $K_0$  is the value corresponding to the system working at the designed operating point and  $K_0+K_1$  acts when the system is far from the operating point. This is reached for example by implementing  $g(e)$  using a hyperbolic secant function like

$$g(e) = 2 - \operatorname{sech}(K_2 e). \quad (3)$$

In case of a sigmoidal function, it could be

$$g(e) = 2 \operatorname{sigm}(K_2 |e|). \quad (4)$$

In both cases, the constant  $K_2$  defines the rate of variation of  $f(e)$ . Fig. 1 shows an example of functions  $f(e)$  and  $g(e)$ .

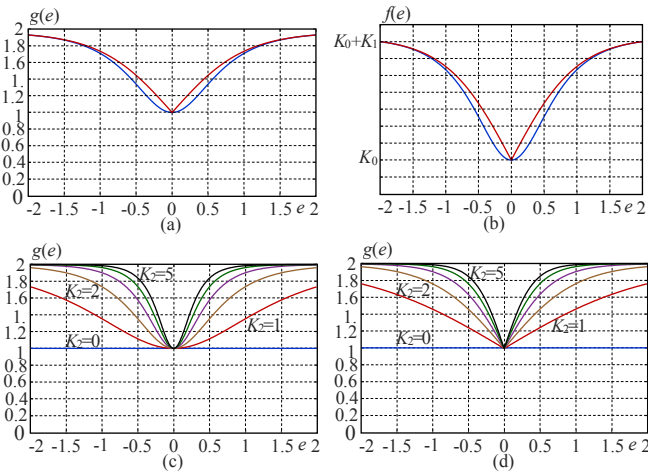


Fig. 1. (a) Basic nonlinear function  $g(e)$ . (b) Scaled nonlinear function  $f(e)$ . (c-d)  $g(e)$  of eqs. (3) and (4) for different values of  $K_2$ .

This approach is limited because all parameters of the PID controller are multiplied by the same nonlinear function. However, the parameters of a PID controller satisfy different objective and therefore should be modified in different ways. Thus, the parameters of a PID controller are individually adjusted by using nonlinear functions in (Taylor & Strobel, 1985) as well as in (Isayed & Hawwa, 2007).

### 2.2 Extended Nonlinear PID

More flexible nonlinear PID approaches include individual nonlinear functions for each controller parameters. In (Isayed & Hawwa, 2007), the nonlinear functions are defined as

$$g_p(e) = K_{0p} + K_{1p}(1 - \operatorname{sech}(K_{2p}e)), \quad (5)$$

$$g_i(e) = (1 + e^{-\gamma(\alpha e + \kappa/10)})^{-1} - (1 + e^{-\gamma(\alpha e - \kappa)})^{-1} \text{ and} \quad (6)$$

$$g_d(e) = K_{0d} + K_{1d}(1 - \operatorname{sech}(K_{2d}e)). \quad (7)$$

The exponential functions (6) are illustrated in Fig. 2.

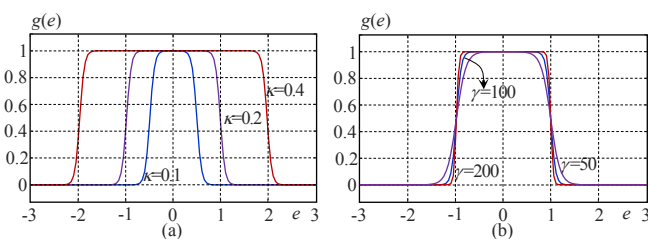


Fig. 2. Exponential function. (a)  $\kappa$  is variable and  $\gamma$  is constant. (b)  $\kappa$  is constant and  $\gamma$  is variable.

The parameters  $\gamma$  and  $\alpha$  are positive constants, which define the shape of the nonlinear function. The exponential function is also used by (Garrido & Soria, 2005) but for the derivative part instead of the integral one.

In (Junoh, et al., 2017), hyperbolic secant functions are used for all parameters of the PID controller, i.e.

$$g_p(e) = K_{0p} + K_{1p}(1 - \operatorname{sech}(K_{2p}e)), \quad (8)$$

$$g_i(e) = 1/[K_{0i} + K_{1i}(1 - \operatorname{sech}(K_{2i}e))] \text{ and} \quad (9)$$

$$g_d(e) = 1/[K_{0d} + K_{1d}(1 - \operatorname{sech}(K_{2d}e))]. \quad (10)$$

### 3. CONTROL STRATEGY OF WIND TURBINES

The control strategy of variable speed wind turbines can be divided in four regions depending on the wind speed. The first region is for a wind speed under the *cut-in* wind speed, where the machine is not able to operate. In the second region, the wind speed is over the *cut-in* but underrated. The control objective is to generate power as much as possible by tracking the optimal generator characteristic. If the wind speed goes over the rated value (region III), the control objective is to maintain constant the power over a wide range of wind speed values by pitching the blades to the feather. Region IV is defined for a wind speed over the cut-off value, where the machine has to be shut down. The transition between regions II and III is sometimes called II  $\frac{1}{2}$  and is characterized by a constant rotor speed. This is illustrated in Fig. 3, according to (Bottasso & Croce, 2009).

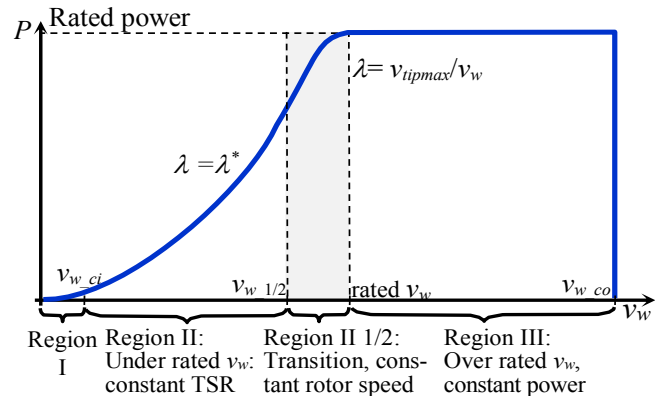


Fig. 3. Control strategy for a variable-speed, horizontal-axis wind turbine

On the other hand, changes in the pitch angle produce disturbances in the thrust force, which in turn increases the amplitude of the fore-aft low damped tower oscillations. In order to increase the tower damping, a proportional feedback control loop from the fore-aft tower speed to the output of the collective pitch controller is proposed in (Bossanyi, 2000). The simple control scheme with both control loops is illustrated in Fig. 4.

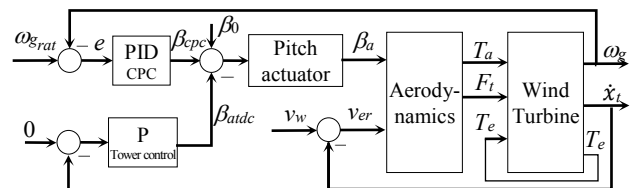


Fig. 4. Control system scheme for a simple pitch control system of a wind turbine

$\beta_0$  is a value for the pitch angle corresponding to the current operating point. It is defined according to the wind speed such

that the rotor speed stays at its rated value. This variable is normally used for the implementation of gain scheduling mechanisms. Variable  $v_{er}$  is a relative wind speed, which is computed as the difference between the effective wind speed and the speed of the tower oscillations.

#### 4. CONTROL SYSTEM IMPLEMENTATION

From Fig. 4, it follows that the complete pitch control system implemented for this work consists of a PID controller and a P controller. For the nonlinear PID controller eqs. (5)-(7) or (8-10) can be used. The nonlinear P controller is implemented by using (5). Consequently, the total number of controller parameters, which have to be found, is 12.

##### 4.1 Controller design by simulation-based parametric optimization

The controller design has two difficulties: On one hand, the number of parameters to be determined is high for a trial and error search. Even the Ziegler-Nichols tuning rules (Åström & Hagglund, 2005) are not adequate here. On the other hand, the model based tuning is also problematic because simple analytical models are inaccurate. Therefore, a simulation-based parametric optimization is used in the present work (see Fig. 5), where the simulation is run in the aero-servo-elastic simulation tool FAST (Jonkman & Buhl Jr., 2005). The vector  $\alpha$  includes all parameters, which have to be obtained.

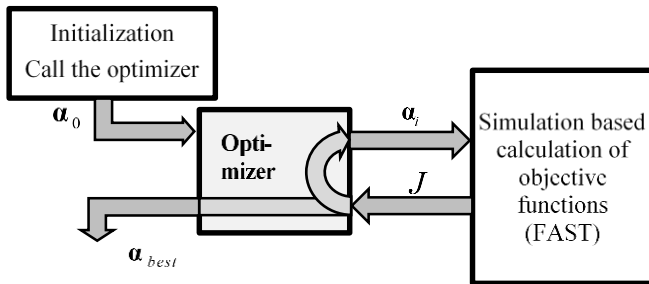


Fig. 5. Scheme on the optimization process

A gradient descent method combined with a constrained active-set algorithm is used as optimizer. The optimization objective is the signed distance between the simulated controlled variable (i.e. rotor speed) and the upper/lower bounds for all time points.

##### 4.2 Optimization process

The parameter optimization process is neither simple nor straightforward. The optimization process is carried out offline. Due to the fact that many parameters are searched that have to satisfy a particular objective and the constraints, there are many parameter sets that will satisfy the optimization conditions and therefore the solution is not unique. In addition, it is also necessary to define start values. Thus, the initialization was carried out by doing a stochastic search, which is stopped at the first occurrence of a stable system.

##### 4.3 Parameter tuning by optimization

It is important to point out first that the NPID can be seen as an extension of the standard PID controller because if the parameters  $K_{1p}$ ,  $K_{1i}$  and  $K_{1d}$  are set to zero, the NPID becomes a PID. Hence, the parameter tuning is done in three stages. In the first stage,  $K_{1p}$ ,  $K_{1i}$  and  $K_{1d}$  are set to zero in order to obtain only values for  $K_{0p}$ ,  $K_{0i}$  and  $K_{0d}$ , i.e. the parameters of a standard PID.

In a second stage, optimal parameters  $K_{0p}$ ,  $K_{0i}$  and  $K_{0d}$  are maintained constant and parameters  $K_{1p}$ ,  $K_{1i}$  and  $K_{1d}$  as well as  $K_{2p}$ ,  $K_{2i}$  and  $K_{2d}$  of the NPID are searched in a second optimization round.

Finally in the third stage, an additional optimization round is started for all parameters. The objective of this additional optimization round is to obtain a fine parameter tuning taking into account possible interactions but starting with the optimal parameters from previous optimization rounds.

#### 5. SIMULATION EXPERIMENTS

##### 5.1 Reference Wind Turbine

In order to study the proposed approach, a reference wind turbine has to be selected. There are several options in the literature, including the 20 MW reference turbine proposed in (Ashuri, et al., 2016), the 10 MW reference turbine from DTU (Bak, et al., 2013) and the 5-MW machine specified in (Jonkman, et al., 2009). However, the 5-MW NREL turbine has frequently been reported in the literature and hence more information about it is available. For this reason, the 5-MW NREL turbine is chosen for the present study. The parameters for the wind turbine are summarized in Table 1.

Table 1. Properties of the 5 MW-NREL Wind Turbine

Parameter	Name	Values	Units
Rotor mass second moment of inertia	$J_r$	38759228	Kg m <sup>2</sup>
Hub mass second moment of inertia	$J_h$	115926	Kg m <sup>2</sup>
Blade mass second moment of inertia	$J_b$	11776047	Kg m <sup>2</sup>
Generator mass second moment of inertia	$J_g$	534.116	Kg m <sup>2</sup>
Equivalent drive train stiffness coeff.	$K_e$	867637000	N m/rad
Equivalent drive train damping coeff.	$D_e$	6215000	N m s/rad
Gearbox ratio	$n_x$	97	
Rated rotor speed	$\omega_{rated}$	1.267109	rad/s
Rated generator torque	$T_{grated}$	43093.55	N m
Tower mass	$m_t$	347460	kg
Tower stiffness coeff.	$K_t$	1439973.74	N/m
Tower damping coeff.	$D_t$	14146.848	N s/m

##### 5.2 Reference Control System

For comparison, the same control system is implemented with the standard PID control algorithms. The number of parameters to be optimized is in this case 6, i.e. from eq. (1)  $K_p$ ,  $K_i$ ,  $K_d$ ,  $b$ ,  $T_1$  and  $T_a$ . For the NPID, the last three parameters are maintained the same.

##### 5.3 Simulation Experiments

The simulation experiments are carried out by using the specialized FAST, which is embedded in a Simulink S-Function. FAST is an aero-servo-elastic code developed by NREL for the simulation of wind turbines (Jonkman & Buhl Jr., 2005). The control system has also been directly implemented in Simulink.

In order to obtain simulation data that can be compared, the wind turbine was operated with constant wind speed. The rated wind speed for this turbine is 11.4 m/s. Hence, the simulation is directly started in Region III at this speed. After some time, the wind speed is set in different simulation experiments to 12, 14, 16, 18 and 20 m/s, respectively. Thus, it is possible to

compare the control performance of both control systems (PID and NPID) for each wind speed.

## 6. SIMULATION RESULTS AND ANALYSIS

### 6.1 Quantitative comparison

In order to do a quantitative comparison between the approaches an average integral of the time-weighted square error (ITSE) is defined. It is important to remark that the simulation-based calculation of the performance indices are time limited and the standard performance indices are evaluated for infinite time. Hence, the performance indices have to be averaged in time (Leondes, 1968). Thus, the finally equation is given by

$$J_{cpc} = \frac{1}{t_{\max} - t_0} \int_{t_0}^{t_{\max}} t [ [\omega_{r, rat}(t) - \omega_r(t)]^2 + [u_{cpc}(t) - u_{cpc}(\infty)]_t^2 ] dt, \quad (11)$$

$$J_{atdc} = \frac{1}{t_{\max} - t_0} \int_{t_0}^{t_{\max}} t [ [x_t(t) - x_t(\infty)]^2 + [u_{atdc}(t) - u_{atdc}(\infty)]_t^2 ] dt, \quad (12)$$

which are computed by the simulation data. In addition, the obtained average energy in kWh is included in the comparison.

**Table 2. Performance index values for different wind speeds**

Approach		12 m/s	14 m/s	16 m/s	18 m/s	20 m/s
$J_{cpc}$	PID	14.45	131.2	24.82	11.08	3.197
	NPID	12.47	12.16	16.65	10.72	2.534
$J_{atdc}$	PID	1.675	0.746	0.171	0.243	0.371
	NPID	1.492	0.733	0.124	0.211	0.207
Energy in [kWh]	PID	963.1	962.9	964.4	964.6	963.6
	NPID	963.2	963.1	964.7	964.9	964.1

Notice that the converted energy is similar for all cases. This is important because it means that no energy loss is remarkable when the NPID is switched on but the control performance is increased: The rotor speed is more stable and the tower is better damped.

### 6.2 Qualitative analysis

The NPID performs better than the PID for all wind speed values, in particular when the operating point is far from the rated values. This is because of two main reasons: the first one is the variable gains that are automatically adapted in a nonlinear way depending on the magnitude of the control error. The second reason is given by the fact that the NPID has many additional parameters to be tuned introducing additional degree of freedom in the optimization process.

However, the introduction of additional parameters leads to more complex optimization process demanding more computational time by each iteration. This aspect is nevertheless compensated because less number of iterations are necessary in order to reach the desired response. In the case of the standard PID controller, less parameters are available for obtaining an acceptable solution and therefore, it is more difficult to arrive to this solution.

In the first simulation experiment, the wind speed is changed from rated value of 11.4 m/s to 12 m/s. Notice that at rated speed there is a switching point, where the control system changes from generator control to pitch control. Therefore, the wind turbine shows at values near to this speed an oscillatory behaviour. Results are presented in Fig. 6 and Fig. 7, where the curves are significantly zoomed for better appreciation.

It is important to clarify that step variations in the wind speed are actually unrealistic. However, this is a very strong requirement for the control system, which has to overcome fast abrupt changes.

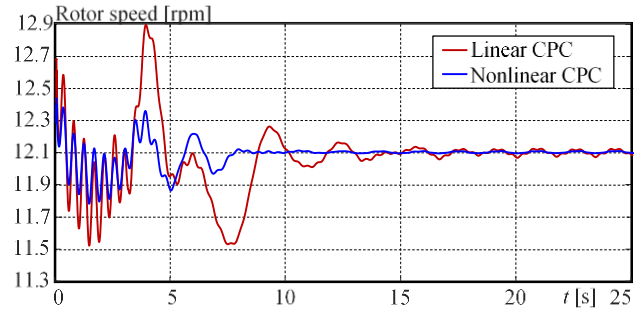


Fig. 6. Rotor speed at a wind speed of 12 m/s

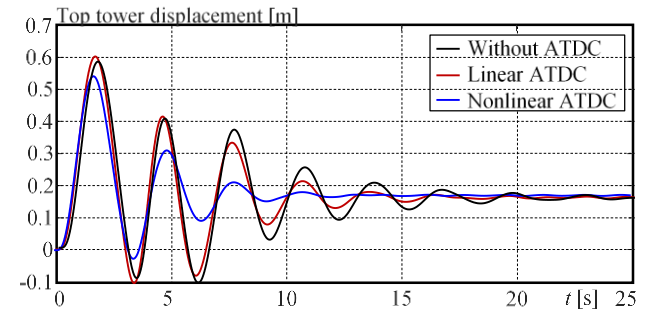


Fig. 7. Tower top displacement at a wind speed of 12 m/s

The figures also show that the standard PID has difficulties to maintain an acceptable level of performance. On the contrary, the NPID is able to maintain a satisfactory behaviour.

Fig. 8 and 9 show the corresponding results for the second simulation experiment, where the wind speed changes from 11.4 to 14 m/s.

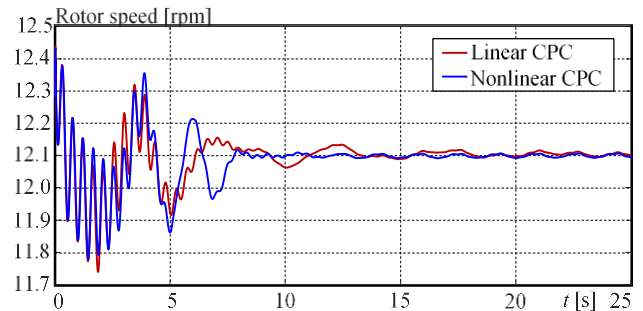


Fig. 8. Rotor speed at a wind speed of 14 m/s

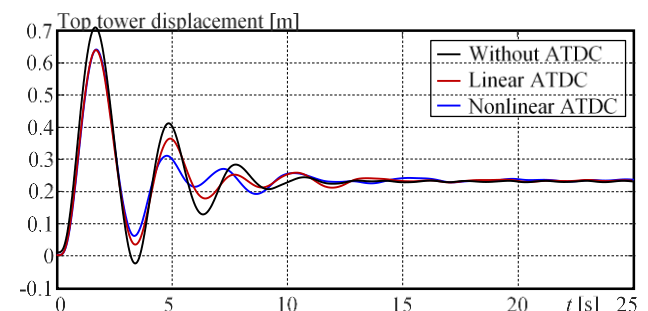


Fig. 9. Tower top displacement at a wind speed of 14 m/s

The next case corresponds to an experiment, where the wind speed is changed from 11.4 to 16.0 m/s. Although the qualitative analysis as well as the signal shapes changes because of

the high wind speed, the control performance is similar to the previous examples. This is illustrated in Fig. 10 and 11.

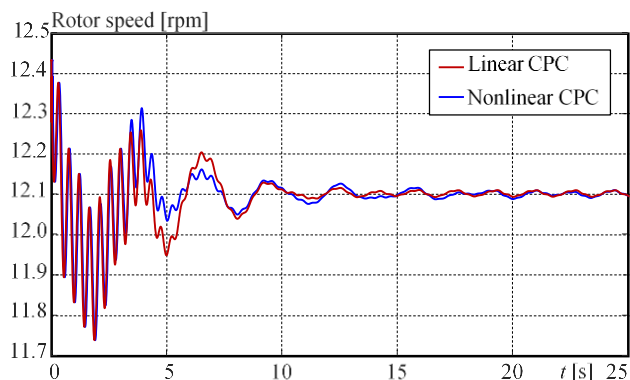


Fig. 10. Rotor speed at a wind speed of 16 m/s

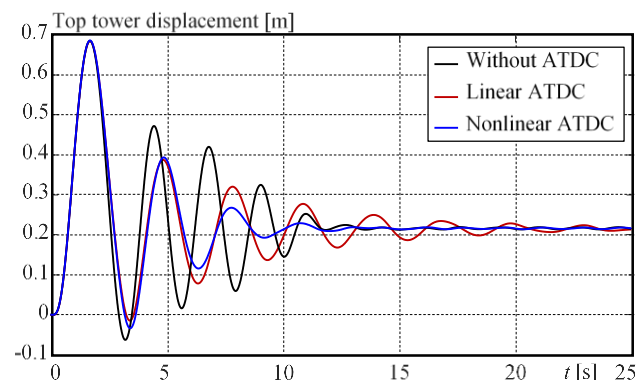


Fig. 11. Tower top displacement at a wind speed of 16 m/s

The last two cases corresponds to wind speed of 18 and 20 m/s. The oscillatory nature of the signals is due to high wind speed.

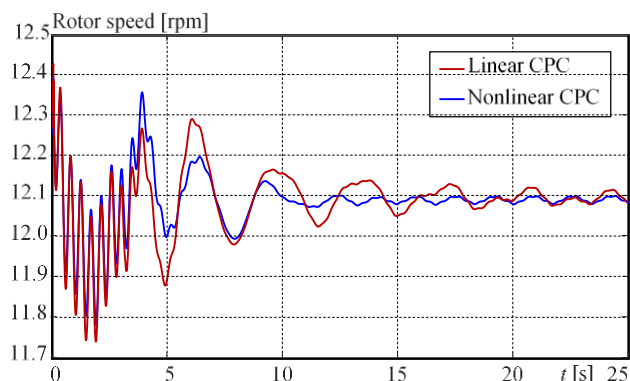


Fig. 12. Rotor speed at a wind speed of 18 m/s

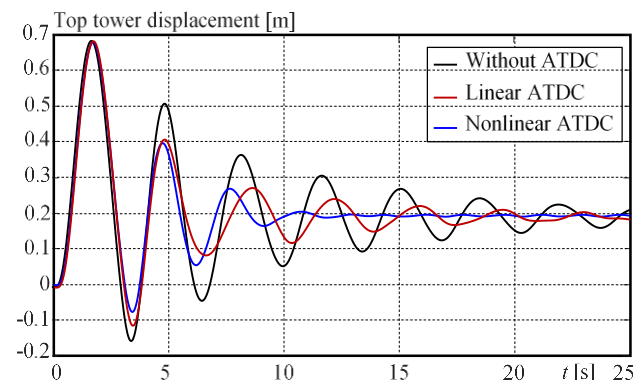


Fig. 13. Tower top displacement at a wind speed of 18 m/s

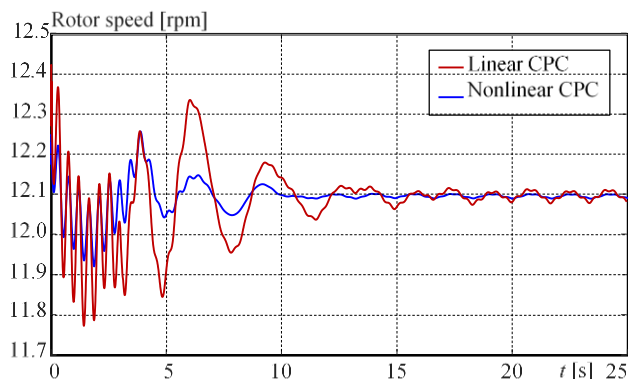


Fig. 14. Rotor speed at a wind speed of 20 m/s

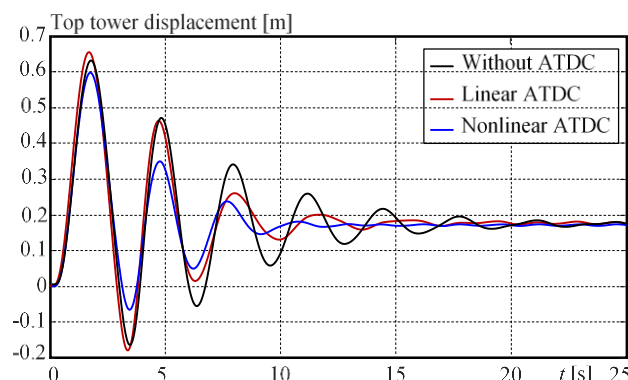


Fig. 15. Tower top displacement at a wind speed of 20 m/s

## 7. CONCLUSIONS

In the present work, preliminary results about the application of a nonlinear PID approach to the pitch control and the active damping tower control of a wind turbine are presented. The first results are very promising given a clear improvement on the control system behaviour.

However, many aspects have to be added to the current development in order to obtain a complete control system suitable for the practical industrial use. First, it is essential to include a gain scheduling mechanism in order to adapt the controller when the operating point changes.

It is also necessary to analyse real wind scenarios such as a full field turbulent wind and extreme operating gusts as well as fatigue loads on the wind turbine and damage equivalent loads. This work has currently been undertaken.

## REFERENCES

- Ashuri, T., Martins, J. R. R. A. & Zaaijer, G., 2016. Aeroservoelastic design definition of a 20 MW common research wind turbine model. *Wind Energy*.
- Åström, K. J. & Hagglund, T., 2005. *Advanced PID control*. s.l.:ISA - The Instrumentation, Systems, and Automation Society.
- Bak, C. et al., 2013. *Description of the DTU 10 MW Reference Wind*, Roskilde: DTU Wind Energy.
- Bossanyi, E., 2000. The design of closed loop controllers for wind turbines. *Wind Energy*, pp. 149-163.
- Bossanyi, E. A., 2003. Wind turbine control for load reduction. *Wind Energy*, p. 229-244.

- Bottasso, C. L. & Croce, A., 2009. *Power curve tracking with tip speed constraint using LQR regulators*, Milano: Politecnico de Milano.
- Burton, T., Jenkins, N., Sharpe, D. & Bossanyi, E., 2011. *Handbook of Wind Energy*. s.l.:Wiley.
- Gambier, A., 2017. *Simultaneous design of pitch control and active tower damping of a wind turbine by using multi-objective optimization*. Kohala Coast, IEEE, pp. 1679-1684.
- Garrido, R. & Soria, A., 2005. Control of a servomechanism using non-linear damping. *Journal of Systems and Control Engineering*, Volume 219, pp. 295-299.
- Isayed, B. M. & Hawwa, M. A., 2007. *A nonlinear PID control scheme for hard disk drive servosystems*. Athens, IEEE.
- Jonkman, J., Butterfield, S., Musial, W. & Scot, G., 2009. *Definition of a 5-MW Reference Wind Turbine for Offshore System Development*, Golden, Colorado: NREL.
- Jonkman, J. M. & Buhl Jr., L. M., 2005. *FAST User's Guide*, Battelle: NREL.
- Junoh, S. C. K. et al., 2017. Nonlinear PID triple hyperbolic controller. *International Journal of Mechanical & Mechatronics Engineering design for XY table ball-screw drive system*, 17(3), pp. 1-10.
- Leithead, W. E. & Domínguez, S., 2004. *Analysis of tower/blade interaction in the cancellation of the tower fore-aft mode via control*. London, EWA.
- Murtagh, P. J., Ghosh, A., Basu, B. & Broderick, B. M., 2008. Passive control of wind turbine vibrations including blade/tower interaction and rotationally sampled turbulence. *Wind Energy*, p. 305–317.
- Seraji, H., 1998. A new class of nonlinear PID controllers with Robotic Applications. *Journal of Robotic Systems*.
- Shahruz, S. M. & Schwartz, A. L., 1993. *Design of optimal nonlinear PI compensators*. San Antonio, IEEE, pp. 3564-3565.
- Su, Y. X., Sun, D. & Duan, B. Y., 2005. Design of an enhanced nonlinear PID controller. *Mechatronics*, Issue 15, p. 1005–1024.
- Taylor, J. H. & Strobel, K. L., 1985. *Nonlinear compensator synthesis via sinusoidal-input describing functions*. Boston, IEEE, pp. 1242-1247.
- Wright, A. D. & Fingersh, L. J., 2008. *Advanced control design for wind turbines*, s.l.: NREL.
- Xu, Y., Hollerbach, J. M. & Ma, D., 1995. A nonlinear PD controller for force and contact transient control. *IEEE Control Systems Magazine*, pp. 15-21.

#### ACKNOWLEDGEMENTS

This work is financed by the Federal Ministry of Economic Affairs and Energy (BMWi).